Journal of Environmental Management 217 (2018) 447–455

Contents lists available at ScienceDirect

Journal of Environmental Management

journal homepage: www.elsevier.com/locate/jenvman

Research article

Performance of an under-loaded denitrifying bioreactor with biochar amendment

Emily M. Bock*, Brady S.L. Coleman, Zachary M. Easton

Department of Biological Systems Engineering, 200 Setiz Hall (0303), 155 Ag Quad Lane, Virginia Tech, Blacksburg, VA 24061, USA

ARTICLE INFO

Article history:
Received 23 February 2018
Received in revised form
21 March 2018
Accepted 25 March 2018

Keywords:
Denitrifying bioreactor
Mid-Atlantic
Nitrate
Biochar
Tile drainage

ABSTRACT

Denitrifying bioreactors are recently-established agricultural best management practices with growing acceptance in the US Midwest but less studied in other agriculturally significant regions, such as the US Mid-Atlantic. A bioreactor was installed in the Virginia Coastal Plain to evaluate performance in this geographically novel region facing challenges managing nutrient pollution. The 25.3 m^3 woodchip bed amended with 10% biochar (v/v) intercepted subsurface drainage from 6.5 ha cultivated in soy. Influent and effluent nitrate-nitrogen (NO_3–N) and total phosphorus (TP) concentrations and flowrate were monitored intensively during the second year of operation. Bed surface fluxes of greenhouse gases (GHGs) nitrous oxide (N_2O), methane (CH_4), and carbon dioxide (CO_2) were measured periodically with the closed dynamic chamber technique. The bioreactor did not have a statistically or environmentally significant effect on TP export. Cumulative NO_3–N removal efficiency (9.5%) and average removal rate (0.56 ± 0.25 g m^{-3} d^{-1}) were low relative to Midwest tile bioreactors, but comparable to installations in the Maryland Coastal Plain. Underperformance was attributed mainly to low NO_3–N loading (mean 9.4 ± 4.4 kg ha^{-1} yr^{-1}), although intermittent flow, periods of low HRT, and low pH (mean 5.3) also likely contributed. N removal rates were correlated with influent NO_3–N concentration and temperature, but decreased with hydraulic residence time, indicating that removal was often N-limited. GHG emissions were similar to other bioreactors and constructed wetlands and not considered environmentally concerning. This study suggests that expectations of NO_3–N removal efficiency developed from bioreactors receiving moderate to high NO_3–N loading with influent concentrations exceeding 10–20 mg L^{-1} are unlikely to be met by systems where N-limitation becomes significant.

© 2018 Elsevier Ltd. All rights reserved.

1. Introduction

Artificial drainage of poorly-drained soils increases agricultural productivity and promotes soil conservation, but elevated concentrations of nitrogen (N) and phosphorus (P) are often detected in drainage waters. A large body of research links agricultural drainage to increased N and P export to water bodies and resultant water quality degradation (e.g., David et al., 2015; Dinnes et al., 2002; Ikenberry et al., 2014). Agricultural nutrient losses are exacerbated by accelerated removal of water from the soil profile via both surface (ditches) and subsurface (tile) drainage, which reduces the opportunity for plant uptake, soil sorption, and nutrient cycling. With over 36.8 million ha of tile-drained cropland in the US according to the 2012 census of agriculture (USDA NASS, 2012), various best management practices (BMPs) to reduce the water quality impact have been developed, including the use of control structures to adjust in-field water table height, riparian buffers, and denitrifying bioreactors.

Denitrifying bioreactors are structural BMPs that intercept N-enriched drainage water and support naturally-occurring soil microorganisms that convert nitrate-nitrogen (NO_3–N) into inert dinitrogen gas (N_2), thereby removing bioavailable N before it enters a water body. This process, heterotrophic denitrification, occurs under anaerobic conditions in the presence of sufficient NO_3–N and organic carbon. Denitrifying bioreactors utilizing woodchip substrate are increasingly accepted drainage BMPs in the Midwest, as evidenced by their incorporation into state-level nutrient reduction strategies in the Upper Mississippi River Basin (IA EPA, 2015; IDALS, 2014; MN PCA, 2014) and the development of a USDA-NRCS conservation practice standard (USDA-NRCS, 2015). However, less work has been done outside of the Corn Belt to evaluate the utility

* Corresponding author.
E-mail addresses: emilyml@vt.edu (E.M. Bock), bscole@vt.edu (B.S.L. Coleman), zeaston@vt.edu (Z.M. Easton).

https://doi.org/10.1016/j.jenvman.2018.03.111
0301-4797/© 2018 Elsevier Ltd. All rights reserved.

of bioreactors in meeting water quality goals in other agriculturally significant areas of the United States. This work contributes to early efforts to adapt bioreactors to agricultural systems in the Mid-Atlantic to meet Chesapeake Bay water quality improvement goals.

Expanding on previous research on biochar-amended woodchip bioreactors (Bock et al., 2015, 2016; Easton et al., 2015), a field-scale woodchip bioreactor with a 10% (v/v) addition of pine-feedstock biochar was installed in a high-priority nutrient management area in Virginia identified by the Chesapeake Bay Total Maximum Daily Load (TMDL). Biochar was selected as a supplemental source of organic carbon based on evidence from laboratory-scale experiments that biochar amendment reduces N_2O production and increases N and P removal in woodchip bioreactors (Bock et al., 2015; Easton et al., 2015), and the results of a pilot-scale experiment suggesting that biochar may increase N removal with moderate to high influent NO_3–N concentrations (>10 mg L^{-1}). The bioreactor was monitored from March 2015 to December 2016 to quantify NO_3–N removal, total P (TP) removal, and emissions of the greenhouse gases (GHGs) nitrous oxide (N_2O), methane (CH_4), and carbon dioxide (CO_2). This system provides a unique case study of bioreactor performance at the lower limits of N loading and pH reported in the literature that is pertinent to adapting bioreactor designs to US Mid-Atlantic agroecosystems. However, while the application is targeted to address a regional water quality issue, this use of a bioreactor with a relatively small drainage network and acid soils has relevance beyond the United States to similar agricultural landscapes. Additionally, this work is among the early investigations of biochar amendment in field-scale bioreactors, along with Hassanpour et al. (2017) and Pluer et al. (2016).

2. Materials and methods

2.1. Site description and bioreactor design

A denitrifying bioreactor was installed in August 2014 to treat subsurface drainage on a farm located in the tidal portion of the Rappahannock River Basin in Middlesex County, VA, in the Coastal Plain physiographic region. The bioreactor is 25.3 m^3 and intercepts a 15.24 cm (6 in) terra cotta tile drain serving as the outlet to a 6.5 ha drainage area. The drainage area is comprised of acid soils (pH 4.6–5.1), approximately 60% of which are poorly drained (30% Myatt loam and 30% an equal mixture of Bertha and Daleville loams), while the remaining 40% are moderately well drained (20% Slagle silt loam, 15% Nansemond loamy fine sand, and 5% other [Soil Survey Staff, accessed 4/6/2017]). The field was planted in soy 2014 to 2016, and per agronomic recommendations no fertilizer was applied.

The bioreactor is approximately 5.8 m long, 5.3 m wide, and 0.8 m deep. The sides and bottom of the bed are lined with impermeable polyethylene, and the top is covered with permeable landscaping fabric. The bed was not covered with a layer of soil, as is typical, to maximize the potential for GHG emissions and reduce the chance of underestimating fluxes from a limited number of measurements. Water-level control structures (AgriDrain Corp.) connect the tile to the bed at the inlet and govern flow at the outlet by the positioning of removable stoplogs. To minimize preferential flow and maximize effective volume, the influent is distributed by a manifold that spans the width of the bed, which consists of 15.24 cm (6 in) PVC pipe with 0.6 cm (0.25 in) perforations connected by a tee to the inlet control structure. During installation, the bed was filled with 90% locally sourced mixed hardwood woodchips and 10% biochar (v/v), which was incorporated with the woodchips as they were added (Biochar Solutions Inc., Carbondale, CO). The biochar, which previously had been demonstrated to enhance NO_3–N removal (Bock et al., 2016), was produced from a pine feedstock via a two-stage pyrolysis where feedstock is held for <1 min at 500–700 °C under low oxygen conditions, after which the temperature is reduced to 300–550 °C and held for up to 14 min. The final product consists of two size fractions produced by passing the biochar through an auger, yielding a material consisting of about 80% particles approximately 1.5 cm long by 1 cm wide by 0.5 cm and 20% as a fine dust fraction on the order of 10–100 μm.

2.2. Data collection

2.2.1. Water chemistry monitoring and sampling

Aqueous grab samples were collected in triplicate from both flow control structures and a piezometer within the bed approximately every two to four weeks between December 2014 and November 2016 on a total of 31 occasions (on 8 others the bed was dry). An automated monitoring and sampling system installed April 2015 collected flow-weighted inlet and outlet water samples and recorded rainfall and bed outflow, on 15- to 60-min intervals. The automated system consisted of two 24-bottle autosamplers (6712, Teledyne Isco); a rain gauge (674 module, Teledyne Isco); pressure transducer (720 module, Teledyne ISCO) installed in the outlet control structure; and a power source consisting of two deep cycle marine batteries in parallel recharged by a 110-W solar panel. Additionally, two capacitance probes (WT-HR Data Logger, TruTrack, Intech Instruments LTD) recorded water levels and temperatures in the inlet and outlet control structures at 15- to 30-min intervals.

Detected flow triggered simultaneous sampling from the inlet and outlet at a rate of one 200 ml sample per every 5 m^3 of effluent, with four 200 ml samples per 1000 ml bottle. Fresh sample bottles were prepared with 5 ml of 10% concentrated sulfuric acid (H_2SO_4) to achieve a sample pH < 2 and prevent degradation at ambient temperature following the method of Burke et al. (2002). Testing of field spikes and comparison with refrigerated samples provided evidence that the acid preservation ensured stable NO_3–N and TP concentrations for up to two weeks in the field (data not shown). Grab samples were field-filtered with 0.45 μm nylon filters, transported on ice, and subsequently stored at 4 °C until analyzed, typically within 48 h. Acid-preserved, autosampler-collected samples were transported and stored at ambient temperature until adjusted to neutral pH with 0.5 M sodium hydroxide (NaOH) solution using an autotitrator (Easy pH Titrator System, Mettler Toledo), after which they were filtered and analyzed or stored at 4 °C until analysis. Samples collected between January and March 2015 were analyzed colorimetrically by spectrophotometer (Thermo Scientific Orion AquaMate 7000 Vis Spectrophotometer) to quantify combined NO_3–N and nitrite-nitrogen (NO_2–N), collectively NOx–N, (chromotropic acid method, Orion AQUAFast method ACR007) and TP (ascorbic acid/persulfate digestion method, ACD095). Beginning April 2016, samples were analyzed by flow injection analysis (FIA, QuikChem 8500, Lachat Instruments) with the cadmium reduction method for NO_x (Lachat method 10-107-04-1-A) and the ascorbic acid method with prior persulfate digestion for TP (Lachat method 10-115-01-4-C). A subset of the grab samples was analyzed for ammonium (NH_4–N) with the salicylate method by either spectrophotometer (ACR012) or FIA (10-107-06-5-J) but were consistently below the method detection limit (0.1 mg L^{-1}), so quantification was discontinued. Note that in subsequent discussion NO_x–N will be referred to as NO_3–N, because NO_2–N is relatively unstable and NO_3–N is the dominant form of dissolved N observed in tile drainage waters (Williams et al., 2015). Additionally, because all samples were filtered prior to analysis, TP more precisely refers to total filterable phosphorus.

2.2.2. Greenhouse gas flux measurement

In December 2015, three soil collars were installed in a row perpendicular to the direction of flow 1.9 m upstream from the outlet water control structure, centered along the width of the bioreactor. Collars consisting of 0.5 m lengths of 25.4 cm (10 in) i.d. schedule 40 PVC were installed to a depth of approximately 30 cm and refilled with the displaced substrate to a height level with the bed surface. GHG fluxes from were measured on 15 occasions between January and October 2016 using the closed dynamic chamber technique (e.g., Collier et al., 2014) with a gas concentration analyzer employing cavity ring-down spectroscopy technology (Model G2508, Picarro, Inc.). The first measurements occurred four weeks after installation to minimize the effect of the resultant disturbance. Briefly, each soil collar was capped to create a closed system, and the headspace was pumped through the inline analyzer and returned to the column, producing a time series of N_2O, CH_4, and CO_2 concentrations (dry molar fractions) from which fluxes were calculated. The inlet and exhaust lines connecting to the analyzer were each 15.24 m lengths of 3.2 mm i.d. inert, polyethylene-lined tubing and attached to the collar cap with compression fittings within bulkhead unions installed in the cap with rubber gaskets to prevent leakage. Headspace was pumped from the top of the collar headspace, through the analyzer, returned via the exhaust line, and discharged from an L-connector near the soil surface pointed away from the intake to prevent short circuiting the flow. The collar was vented by disconnecting the inlet line during capping to minimize changes in pressure that would affect the concentration gradients of analyte gasses (de Klein and Harvey, 2012). Before reconnecting the inlet line to measure headspace GHG concentrations, a wide elastic band was secured around the overlap of the cap and collar to create a gastight seal. Ambient air was pumped through the instrument between measurements for five minutes to allow a complete return to background concentration prior to measuring flux from the next collar. To calculate analyte mass concentrations from dry molar fractions, the air temperature and barometric pressure were recorded during flux measurements with respective accuracy of ± 0.2 °C and ± 0.8 kPa. Fluxes were consistently measured at midday, within a window about 12:00 to 14:00, to minimize variation due to diurnal patterns in GHG flux, recognizing that this window likely captures fluxes slightly greater than the daily average expected to occur between 10:00 and 12:00 (de Klein and Harvey, 2012).

2.3. Data processing and calculations

All calculations and subsequent statistical analyses were performed using the R language and environment for statistical computing (R Core Team, 2017).

2.3.1. Nutrient loading and removal

Nutrient loading and removal were assessed for a one-year period beginning 13 mo after bioreactor installation, September 2015 to September 2016, when aqueous samples were collected with sufficient frequency. Nutrient concentrations were quantified in at least one sample from the inlet and outlet on 42% and 46% of the days in this observation period for NO_3–N and TP, respectively. Daily average concentrations were used for calculations when multiple concentration measurements were available for a given day. Nutrient concentrations determined with different analytical methods (e.g., spectrophotometer and FIA) were treated as equivalent based on comparative testing of a subset of samples (data not shown). Samples below the method detection limit were assigned as half of that concentration, 0.01 mg L^{-1} for TP quantified by FIA and 0.06 mg L^{-1} for TP quantified by spectrophotometer; NO_3–N concentrations of all samples exceeded the detection limit. Flow rates were calculated from pressure transducer measurements of nappe height using an equation calibrated specifically for the AgriDrain 45° degree v-notch weir:

$$Q = 1.7406H^{1.953} \quad (1)$$

where Q (L min^{-1}) is the flow and H (cm) is the nappe over the v-notch, which is valid for the flows encountered, within the 5–153 L min^{-1} (Partheeban et al., 2014). The daily drainage volume passing through the bed was calculated by summing the product of measured flow rates and time elapsed between measurements. Daily nutrient mass loading and removal rates (g m^{-3} d^{-1}) were calculated by multiplying the daily drainage volume by the influent concentration or influent less effluent concentration, respectively, and normalized to total bed volume (25.3 m^3). For evaluation of the relationship between removal rates and bed conditions, actual daily removal rates were estimated on the basis of saturated rather than total bed volume using water heights recorded by the pressure transducers.

2.3.2. Greenhouse gas flux

The volumetric concentrations recorded by the GHG analyzer were converted to mass concentrations (mg m^{-3}) using the ideal gas law and ambient temperatures and pressures recorded during measurements (Collier et al., 2014). Fluxes were calculated from chamber headspace concentration time series using two methods, linear regression (LR) and a physically-based, non-steady-state diffusive flux estimator (NDFE) developed by Livingston et al. (2006). The NDFE method estimates pre-deployment flux by applying Fick's Law, assuming vertical gas transport, soil matrix homogeneity, and a trace gas source supplying a constant, positive flux under undisturbed conditions. The collar design restricting horizontal gas movement and the relative uniformity of the woodchip mixture were thought to adequately satisfy these assumptions.

First, fluxes were calculated by LR as:

$$F = S \cdot V \cdot A^{-1} \quad (2)$$

where F (g m^{-2} s^{-1}) is surface flux, S (g m^{-3} s^{-1}) is the slope of the analyte concentration regressed over time, V (m^3) is total volume of the recirculating system, and A (m^2) is the surface area contained in the soil collar (Duran and Kucharik, 2013). Next, all non-negative LR fluxes were also estimated with the NDFE method (26 of 45 for N_2O, 37 of 45 for CH_4, and all CO_2 measurements). GHG concentration curves were fit to the NDFE equation (Eq. (3)) with the Levenberg-Marquardt modification to the least-squares algorithm:

$$C_t = C_0 + f_0 \tau \left(\frac{A}{V}\right)\left[\frac{2}{\sqrt{\pi}}\sqrt{t/\tau} + \exp(t/\tau) erfc\left(\sqrt{t/\tau}\right) - 1\right] \quad (3)$$

where C_t (g m^{-3}) is headspace concentration at a given time, t (s), f_0 (g m^{-2} s^{-1}) is pre-deployment flux, C_0 (g m^{-3}) is background trace gas concentration, τ (s) is an experimental constant representing the time until the concentration gradient in the chamber decreases to zero as headspace concentration increases, A and V are as defined above, and *erfc* is the complimentary error function. Starting values of f_0 are assigned as the LR flux calculation and for τ as $(V/A)^2/D$, where D (m^2 s^{-1}) is the diffusivity of the trace gas in air.

NDFE was the preferred flux calculation method because LR can substantially and systematically underestimates trace gas flux when responses are nonlinear (Duran and Kucharik, 2013; Kutzbach et al., 2007; Livingston et al., 2006). NDFE estimates were used for subsequent analysis of CO_2–C and CH_4–C flux, except for four very low magnitude negative CH_4–C fluxes calculated by LR

(net transfer into the bed, −0.1 to 0.0 mg m^{-2} d^{-1}), which violated the NDFE assumption of positive flux. LR calculations were determined to be reasonably accurate for low magnitude fluxes by comparing calculated values for the ten lowest but positive CH_4–C fluxes. For N_2O–N, LR was determined to be more appropriate because absolute flux values were several orders of magnitude smaller than the CO_2 and CH_4 fluxes that produced nonlinear responses and over 30% of measurements were negative. Additionally, the low signal to noise ratio of the headspace response, N_2O–N having the lowest atmospheric concentration among the analytes, adversely affected NDFE calculations. However, NDFE was used to calculate the two largest N_2O–N fluxes because nonlinearity was visually apparent. To estimate the N_2O emission factor, the proportion of removed NO_3–N emitted as N_2O–N, the average flux among the three collars was extrapolated to the entire bed surface area (30.9 m^2) for a 24 h time period and compared to the daily cumulative NO_3–N removal.

2.4. Statistical analysis

Removal rates of NO_3–N and TP were calculated from the irregularly spaced time series of flow and nutrient concentration measurements collected during the second year of operation (mo 13–26). The statistical significance and 95% confidence intervals of mean removal rates were determined with one-sample t-tests. Removal rates were also evaluated separately for the growing (April 10 to September 29, 2016) and non-growing (September 30, 2015 to April 9, 2016) seasons. The difference in average seasonal loading and removal were evaluated with an unpaired two-sample *t*-test. Anticonservative p-values were corrected for serial correlation after Ghane et al. (2016) by adjusting the standard error:

$$SE = \sqrt{\frac{1+r_1}{1-r_1}}\frac{s}{\sqrt{n}} \quad (4)$$

where s is the standard deviation of the measured removal rates, n is the sample size, and r_1 is the correlation coefficient at lag 1 of a first order autoregressive model (AR1). N and P removal rates were determined to be appropriately represented by AR1 models because their partial autocorrelation functions were below the $\alpha = 0.05$ significance level after the first lag. Removal rates were determined to be stationary by the Durbin Watson test.

The effects of influent concentration, hydraulic residence time (HRT), and temperature on nutrient removal rates were examined with a linear model fit by generalized least squares (GLS). The model was fit using 118 days of data collected during a subset of the monitoring period (January 16 to October 4, 2016, mo 17–26) for which saturated volume was also recorded. Independent variables were centered prior to regression, and the serial correlation of errors over time was modeled as continuous AR1. Model parameters were selected by comparing nested models with the log likelihood ratio test, beginning with maximal model including all interaction effects and iteratively removing non-significant terms. Homoscedasticity was verified by visually examining the distribution of residuals relative to fitted values, and variance inflation factors <2.6 indicated an acceptable degree of collinearity among the independent variables. Model residuals were not normally distributed, but this assumption is the least critical, especially for describing relationships between the explanatory and dependent variables as opposed to predicting responses under specific conditions (Gelman and Hill, 2007, p. 46). Statistical significance of explanatory variables and of individual parameter coefficient estimates was determined with the F-test with marginal sum of squares and Wald *t*-test, respectively.

The effect of in-bed conditions on surface emissions of N_2O, CH_4, and CO_2 was similarly characterized with the GLS modeling procedure. Flux models included the continuous AR1 correlation structure and the same, centered independent variables, along with collar position. However, interaction effects were not evaluated due to the small size of the dataset (N_2O and CO_2 n = 36, CH_4 n = 35). Measurements from 3 of the 15 measurement dates (June 29, August 24, and September 21, 2016) were excluded due to the absence of flow through the bioreactor, and an additional single measurement of CH_4 on June 15, 2016 was excluded due to poor data quality. Additionally, to meet assumptions of homoscedasticity and normality of errors, the natural log transformation was applied to CH_4 and CO_2 flux measurements; a small offset was added to eliminate negative CH_4 values, representing net transfer into the bed, prior to taking the logarithm. A cubic root transformation, preserving mathematical sign, was applied to N_2O since a significant proportion of fluxes were negative, precluding the more common logarithmic transformation. Equal variance among the collars was confirmed by the Levene test.

3. Results and discussion

3.1. Nutrient loading and removal

The bioreactor cumulatively removed an estimated 9.5% of the influent NO_3–N at an average rate of 0.56 ± 0.25 g m^{-3} d^{-1} during the second year of operation, but was unsuccessful in removing TP (Fig. 1, Table 1). TP removal was not statistically significant during the observation period ($p = 0.2082$), nor during the growing ($p = 0.8003$) or non-growing season ($p = 0.2354$) when evaluated separately. These results corroborated the findings of Christianson et al. (2011) in laboratory tests and Pluer et al. (2016) in field-scale bioreactors that biochar addition does not enhance P removal. The lack of response to biochar amendment emphasizes the limited relevance to field-scale, flow-through systems of an earlier batch experiment, which suggested biochar enhanced P removal (Bock et al., 2015). However, each of the authors investigated different biochars, highlighting the potential for considerable variability in biochar properties. Nonetheless, given that TP concentrations were below the limit of quantification in approximately 30% and 22% of the influent and effluent samples, respectively (Fig. 1), it is unsurprising that no statistical difference was found between inlet and outlet concentrations despite the flow-weighted average concentrations being slightly lower at the outlet (Table 1). Although the effect of biochar on NO_3–N removal could not be determined by this study, recent work suggests that due to consumption of its labile organic carbon (i.e., aging) biochar may only enhance NO_3–N removal in woodchip bioreactors during the first several years of operation (Hassanpour et al., 2017). Additionally, the low influent NO_3–N concentrations (flow-weighted mean 3.7 mg L^{-1}) may influence the effectiveness of biochar in removing N. Findings from the field-scale study of Hassanpour et al. (2017) were consistent with the pilot-scale experiment of Bock et al. (2016) that indicated NO_3–N removal in biochar-amended bioreactors only exceeds that of the woodchip systems when influent concentrations exceed 5 mg L^{-1} at lower temperatures and 10 mg L^{-1} at higher temperatures.

The mean NO_3–N removal rate was statistically significant ($p < 0.001$) and seasonally constant, but N removal efficiency was substantially greater during the growing (20.4%) than the non-growing season (5.4%). The overall 9.5% removal efficiency failed to meet the NRCS target of 25–45%, but load reduction was similar to the lower limit of the 9.0–62% range of removal efficiencies observed in three tile bioreactor in the Maryland Coastal Plain (Rosen and Christianson, 2017). Likewise, the range of observed

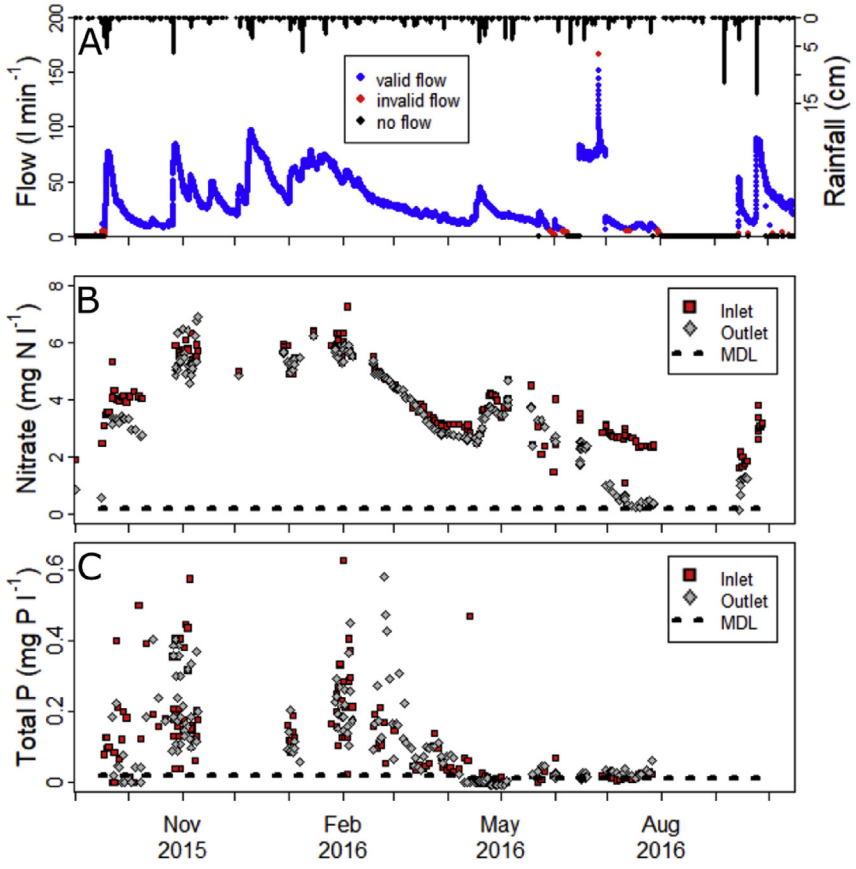

Fig. 1. a-c. Measured flowrate of water leaving the bioreactor and daily rainfall (a); concentrations of nitrate-nitrogen (b) and total phosphorus (c) in bed influent and effluent water samples. Dashed lines represent method detection limits (MDL). [figure sizing: 2 columns].

Table 1
Mean and 95% confidence interval ($\alpha = 0.05$) of nutrient loading rate, bed-normalized removal rate, and flow-weighted influent and effluent concentrations. All values are included for nitrate-nitrogen, but removal rates for total phosphorus are not reported because they are not statistically significant. Annual values are seasonally-weighted based on the duration of the growing (April 10 to September 29, 2016) and non-growing seasons (September 30, 2015 to April 9, 2016).

NO_3–N		Annual	Growing 1	Non-growing
Loading	kg ha^{-1} yr^{-1}	8.5 (4.1–12.9)	4.0 (2.5–5.5)	14.2 (7.8–20.6)
	g m^{-3} d^{-1}	6.0 (2.9–9.1)	2.8 (1.7–3.9)	10.0 (5.5–14.5)
Removal	g m^{-3} d^{-1}	0.56 (0.31–0.81)	0.56 (0.34–0.82)	0.57 (0.24–0.91)
Conc.	inlet mg L^{-1}	3.7 (2.8–4.6)	2.9 (2.4–3.4)	4.7 (3.6–5.7)
	outlet mg L^{-1}	3.1 (1.8–4.4)	2.1 (0.1–4.2)	4.4 (3.3–5.5)
Total P		**Annual**	**Growing 1**	**Non-growing**
Loading	kg ha^{-1} yr^{-1}	0.19 (0.05–0.33)	0.04 (0.00–0.08)	0.48 (0.22–0.73)
	g m^{-3} d^{-1}	0.27 (0.07–0.47)	0.03 (0.00–0.05)	0.34 (0.16–0.51)
Conc.	inlet mg L^{-1}	0.13 (0.08–0.20)	0.03 (−0.01 to 0.07)	0.19 (0.13–0.25)
	outlet mg L^{-1}	0.03 (0.07–0.18)	0.02 (0.00–0.04)	0.17 (0.11–0.23)

NO_3–N removal rates, −2.25 to 8.10 g m^{-3} d^{-1}, was similar to that of the Maryland bioreactors, 0.21–5.36 g m^{-3} d^{-1} (Rosen and Christianson, 2017), apart from the net export observed during 17% of the days when both influent and effluent samples were collected. However, on over half of the days during which NO_3–N export occurred, the difference between influent and effluent concentrations was <0.2 mg L^{-1}, suggesting increasing uncertainty in calculation of low magnitude removal or export as the difference between influent and effluent concentrations decreases. Bioreactor performance was also comparable, although somewhat weaker, to a ditch diversion bioreactor also located in the Maryland Coastal Plain, where NO_3–N removal rates averaged 0.97 g m^{-3} d^{-1} and load reduction was 25% (Christianson et al., 2017). Although, the average NO_3–N removal rate was well short of the 95% confidence interval (CI), 2.9–7.3 g m^{-3} d^{-1}, for average bioreactor performance reported in a recent meta-analysis by Addy et al. (2016), performance was likely constrained by influent concentration, HRT, and bed age, which the meta-analysis identified as significant controls on removal.

The magnitude and seasonal distribution of NO_3–N loading constrained the performance of the bioreactor. The average annual NO_3–N loading rate of 9.4 kg ha^{-1} yr^{-1} was less than 30% of that reported as representative of Midwestern tile drainage, 31.4 kg ha^{-1} yr^{-1} (Christianson et al., 2013a), resulting in an average flow-rated influent NO_3–N concentration of only 4.37 mg L^{-1} (Table 1). Noting that the bioreactor meta-analysis found that

influent NO_3–N concentration significantly influences the removal rate, the category of bioreactors receiving low NO_3–N influent (<10 mg L^{-1}), which averaged 2.4 mg L^{-1} (95% CI 1.0–4.9), provides a more appropriate comparison (Addy et al., 2016). Additionally, the seasonal distribution of loading constrained NO_3–N removal more severely than would be predicted by the annual average, which decreased sharply during the growing season to only 3.9 kg ha^{-1} yr^{-1} (2.8 g m^{-3} d^{-1} on the basis of bed volume). Consequently, N-limited conditions, defined as effluent NO_3–N <1 mg L^{-1} (e.g., Elgood et al., 2010), occurred during nearly 20% of the observation period exclusively during the growing season in July, August, and September. Both greater influent NO_3–N concentrations (Table 1) and drainage volumes (Table 2) during the non-growing season drove seasonal differences in loading, as can be seen in Fig. 1, and the flow-weighted influent concentration was 63% higher than during the growing season. However, despite these seasonal differences in loading, the NO_3–N removal rate remained constant, reflecting the constraint of lower temperatures during the non-growing season, which are also associated with higher influent dissolved oxygen concentrations. Indeed, the "design and operational challenge" posed by springtime higher NO_3–N loads and drainage volumes coinciding with low removal due to decreased residence times and lower temperatures has been noted elsewhere (e.g., Christianson et al., 2013a).

GLS analysis revealed a significant correlation between the NO_3–N removal rate and influent NO_3–N concentration (Table S1), providing additional evidence supporting the conclusion of Addy et al. (2016) that N-limitation may need to be considered for bioreactor design, although NO_3–N removal has often been considered a zero-order kinetic reaction. As expected, temperature was also significantly correlated with the NO_3–N removal rate, as has been reported for many bioreactors. Notably, the effect of both influent concentration and temperature on NO_3–N removal were found to decrease as HRT increased. For example, a 1 mg L^{-1} increase in influent concentration for a 4 h HRT is associated with an increase in removal by about 2.76 ± 0.59 g m^{-3} d^{-1}, but if HRT is lengthened to 10 h the same change in concentration produces only a 1.25 ± 0.18 g m^{-3} d^{-1} increase in removal. For temperature, a 5 °C increase with a 4 h HRT is associated with an increase in NO_3–N removal of 4.09 ± 0.82 g m^{-3} d^{-1} but only 2.61 ± 0.42 g m^{-3} d^{-1} for a 10 h HRT. The regression coefficient for influent concentration of 1.25 is comparable to the 0.44–1.25 range reported by Christianson et al. (2012), who also observed dependence of NO_3–N removal on influent concentration. Christianson et al. (2012) posited that the nearly 1:1 relationship between influent concentration and removal rate, when averaged across four individual bioreactors, provided strong evidence that first-order kinetics governed N removal. When the GLS model was re-fit excluding days when net NO_3–N export occurred, the coefficient was reduced to 1.02, likewise indicating a first-order reaction. Relative to the range of observed bed conditions (NO_3–N influent 1.77–6.32 mg L^{-1} and 8.1–25.3 °C), changes in influent concentration were associate with larger differences the NO_3–N removal rate than changes in temperature, and both had larger effects for lower HRTs. These significant interaction effects also reflect that removal for this bioreactor is better characterized by first-order kinetics. The removal rate would be expected to be independent of HRT for a zero-order reaction proceeding at a constant rate as NO_3–N concentration declined in the bed. In contrast, with constant temperature and influent concentration, an inverse correlation between HRT and the average removal rate can be explained by a proportional decrease in the instantaneous removal rate as bed concentration decreases, lowering the average removal rate as HRT increases. Findings of Addy et al. (2016) also emphasize the importance of N limitation as a control on NO_3–N removal in bioreactors and suggest that first-order kinetics persist at higher influent concentrations than previously reported. Whereas N-limitation is often defined by effluent NO_3–N < 0.5–1 mg L^{-1} (e.g., van Driel et al., 2006; Elgood et al., 2010), the recent met-analysis found that NO_3–N removal rates were correlated with influent concentration and significantly differed between high (>30 mg L^{-1}), intermediate (10–30 mg L^{-1}), and low (<10 mg L^{-1}) categories (Addy et al., 2016). Therefore, as supported by this GLS analysis, the 20% of daily effluent samples collected during the growing season that had NO_3–N concentrations <1 mg L^{-1} indicate only the minimum duration of N-limited bed conditions in the bed.

In addition to low NO_3–N loading, bioreactor performance was likely also constrained by bed age, HRT, effective volume, and drainage acidity. N removal rates were evaluated during mo 13–26 of operation, which are on average 70% lower than the rates during first year of operation (Addy et al., 2016). While the median HRT of 10.0 h (assuming a porosity of 0.6 based on measurement with volumetric displacement) is thought to be adequate to reach target efficiency of 25–45% removal, 20% of the time HRT was <6 h, corresponding with the meta-analysis average NO_3–N removal rate of only 0.7 g m^{-3} d^{-1} (95% CI 0.3–1.3 [Addy et al., 2016]). While the observed mean NO_3–N removal (0.56 g m^{-3} d^{-1}) was still lower than average for beds with 6–20 h HRTs (4.4 g m^{-3} d^{-1} [Addy et al., 2016]), site constraints necessitating suboptimal bed dimensions may account for the relative underperformance. The bed length to width ratio of 1:1.1 deviates substantially from the recommended minimum 1:5 recommended to avoid preferential flow (Christianson et al., 2013b). Preferential flow, when a substantial portion of the drainage reaches the outlet before the bulk flow, can reduce bioreactor effective volume and cause theoretical HRT calculations to overestimate residence times, though the inlet distribution manifold was intended to mitigate these effects. Additionally, removal rates are reported here on the basis of total bed volume, but an average of only 70% of the bed volume was saturated and actively treating drainage waters. However, extrapolating to full bed utilization would increase mean NO_3–N removal to only 0.85 g m^{-3} d^{-1}. Lastly, bed pH averaged only 5.3, which is typical for the acidic soils of the Atlantic Coastal Plain but well below the optimal pH range or denitrification of 7–8 (Mateju et al., 1992). Although the effect of pH on NO_3–N removal could not be distinguished, lower denitrification rates and greater N_2O production than under neutral pH would be expected (Mateju et al., 1992).

Table 2
Cumulative rainfall and drainage volume flowing through the bioreactor as well as average temperature and flow rate on an annual basis and separated by growing and non-growing season.

		Annual	Growing	Non-growing
Total	drainage (cm)	22.8	6.0	16.8
	rainfall (cm)	151.9	77.4	74.5
Mean	temp (℃)	17.9	21.7	12.5
	flow (L s^{-1})	28.1	15.5	39.3
	pH	5.3	5.2	5.5

3.2. Greenhouse gas flux

Although GHG emissions were highly variable, measured fluxes (Fig. 2) were comparable to those reported for other bioreactors. The range of N_2O–N emissions, −0.60 to 19.7 mg m^{-2} d^{-1}, was similar to the −5.4 to 14.6 mg m^{-2} d^{-1} of a stream-bed bioreactor and emissions from agricultural soils, 0.1–15.0 mg N_2O–N m^{-2} d^{-1} (Elgood et al., 2010). Nearly 90% of measured N_2O–N fluxes were within the range of 0.24–3.12 mg m^{-2} d^{-1} of a tile-fed woodchip bioreactor in Illinois, which the authors considered to be negligible

(Woli et al., 2010). Measured CH_4-C m^{-2} d^{-1} fluxes, 0–125 mg m^{-2} d^{-1}, were also within the range observed by Elgood et al. (2010), −2.6 to 1236 mg m^{-2} d^{-1}, who likewise observed the highest CH_4 production in the warmer summer months (Fig. 2b). Both N_2O–N and CH_4–C fluxes were within the ranges reported in a review of GHG emission from constructed wetlands for wastewater treatment, approximately −0.1 to 21.5 mg m^{-2} d^{-1} and 1–650 mg m^{-2} d^{-1}, respectively, encompassing different wastewater treatment types and environmental conditions (Mander et al., 2014). However, emissions from the bioreactor were generally lower than those reported for the treatment wetlands; the median value for CH_4-C, 150 mg m^{-2} d^{-1}, corresponded with the maximum flux observed from the bioreactor, and the median treatment wetland flux of N_2O-N, 3 mg m^{-2} d^{-1}, was similar to the 90th percentile of flux measurements (Mander et al., 2014). With respect to CO_2, as noted by Schipper et al. (2010), the substrate used in the bioreactor would have decayed and released CO_2 had it been used elsewhere, and thus does not contribute to net CO_2 emissions. However, to assess total GHG emissions from the bed, the combined GHG flux is reported as CO_2 equivalents (CO_2–eq, Fig. 2d), whereby N_2O–N and CH_4–C fluxes are multiplied by their global warming potential over a 100-yr timespan, factors of 298 and 25, respectively (IPCC, 2007). From this perspective, both N_2O and CH_4 contributed substantial portions of total warming potential of GHGs emitted from the bed at certain times. Up to 44% of total CO_2-eq flux of was supplied by N_2O–N, although the average contribution was just over 6%, and CH_4–C accounted for up to 15% of CO_2-eq, but averaged only 3.6%. Calculated CO_2-eq ranged 1.3–166.6 g m^{-2} d^{-1}, over 90% of which was emitted as CO_2–C at an average rate of 0.5–82.3 g m^{-2} d^{-1}.

The proportion of N_2O–N produced by the bioreactor relative to NO_3–N removal provides additional context to determine if emissions are potentially problematic. Point measurements of the N_2O emission factor ranged −3.2 to 3.7% for individual collars and −1.5 to 1.2% for each measurement date; negative emission factors occurred when the bed acted as a sink rather than source of N_2O–N. The overall average emission factor was 0.07%, and the median only 0.01%, both substantially less than the 0.75% determined by the

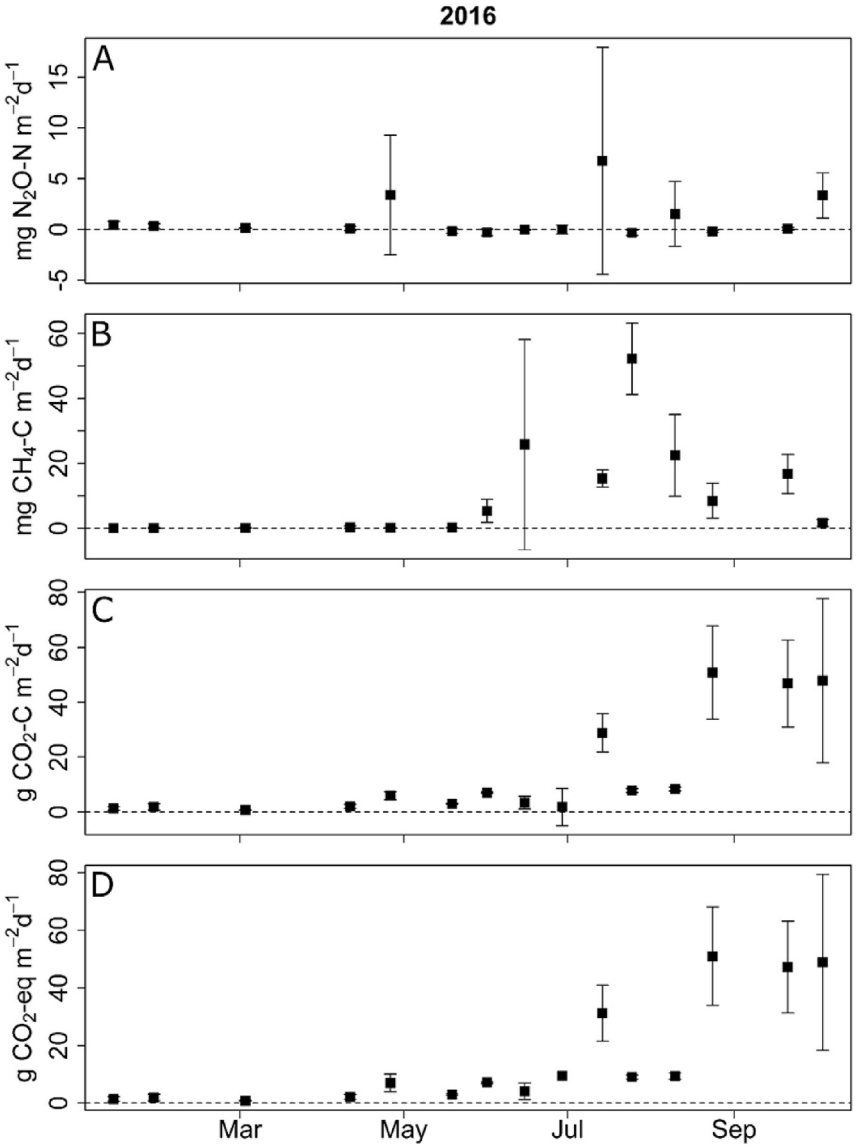

Fig. 2. a-d. Average flux measurements of N_2O (a), CH_4 (b), CO_2 (c), and the combined warming potential of the three gases as CO_2 equivalents (d) from three soil collars installed in a denitrifying bioreactor. Error bars represent ± one standard deviation, and the dashed line is positioned at zero net flux. Note y axes are different scales and units differ between 3a,b (mg m^{-2} d^{-1}) and 3c,d (g m^{-2} d^{-1}). [figure sizing: 1.5 column].

IPCC (2007) for agricultural NO_3–N inputs, suggesting N_2O–N emissions were, on average, mitigated rather than enhanced by the bioreactor. Emission factors reported in the literature vary from 0.6% (Elgood et al., 2010) and 0.84% (Moorman et al., 2010) of removed NO_3–N exported as N_2O–N dissolved in bioreactor effluent, to 0.004% as surface emissions from a field-scale bioreactor (Woli et al., 2010), and 0.003–0.028% emitted in a laboratory column study (Greenan et al., 2009). Findings of Warneke et al. (2011), who observed dissolved export (3.3%) exceeding surface flux (1%) in a bioreactor receiving greenhouse effluent with NO_3–N concentrations >100 mg L^{-1}, suggest that the calculated emission factor depends on the loss pathway quantified and that measuring only gaseous or dissolved flux may underestimate N_2O–N production. However, although dissolved N_2O–N losses were not quantified, and extrapolating measured fluxes over the bed surface area and over time, even only one day, introduces significant uncertainty, N_2O–N emissions form this particular bioreactor did not raise serious concern given the similarity to previously reported emission factors and flux magnitudes. Nonetheless, determining the effect of bed conditions on GHG emissions may identify potentially problematic scenarios.

GLS analysis indicated that influent NO_3–N concentration, HRT, and temperature each had a significant effect on flux of at least one GHG (Table S2). Note these modeled relationships pertain to the range of observed conditions, 3–20 h HRT, 8–25 °C, and 1.8–6.3 mg L^{-1} influent NO_3–N concentration. For N_2O–N, flux was negatively correlated with HRT ($p = 0.0017$), which is likely due to decreasing rates of denitrification over time as NO_3–N is consumed; for a given influent concentration, the NO_3–N removal rate likewise declined as HRT increased. Additionally, shorter HRTs may be associated with higher dissolved oxygen concentrations within the bed, which have been associated with elevated N_2O–N emissions in bioreactors (Elgood et al., 2010). Although influent NO_3–N concentration and temperature had significant effects on NO_3–N removal and were expected to also influence N_2O–N flux, the high variability of N_2O–N flux (300% CV) may have masked these effects. Mander et al. (2014) report a correlation between influent total N and N_2O–N emissions in constructed wetlands, though the relationship with temperature is unclear across the studies reviewed. Different responses to temperature have also been reported for bioreactors, demonstrating the difficulty in isolating the effect of a single variable on emissions. The highest N_2O–N fluxes from were observed in colder months due to elevated dissolved oxygen levels by Elgood et al. (2010) and Moorman et al. (2010), but during the highest temperatures when NO_3-N removal rates were greatest by Warneke et al. (2011). Methane fluxes were strongly correlated with HRT and temperature, a 1 h increase in HRT increasing CH_4–C flux by about 7.7% ± 1.7% (plus or minus one standard deviation of the coefficient estimate) and 1 °C increase in temperature increasing flux by about 12.0 ± 4.0%. While seasonal elevation in CH_4–C flux may be unavoidable due to the dependency on temperature, also observed Elgood et al. (2010), limiting HRTs to avoid excessively reducing conditions favorable to methanogenesis is currently recommended practice. Though the effect of influent NO_3–N concentration on CH_4–C flux was not significant, the correlation with HRT suggests that CH_4–C emissions increase after NO_3-N is depleted, as has been reported previously reported (Elgood et al., 2010). Continued study of GHG emissions in bioreactors might enable a more precise comparison of the NO_3–N removal efficiency gained by increasing HRTs against the additional CH_4 produced. Although bioreactor CO_2–C emissions are considered net neutral, accelerated production may be of interest. Carbon dioxide flux was positively correlated with temperature, each 1 °C associated with a 9.5 ± 2.4% increase in flux, and negatively correlated HRT and influent NO_3–N concentration. An increase in the HRT by 1 h decreases flux by 8.7 ± 1.4% and a 1 mg L^{-1} increase in influent NO_3–N concentration reduces flux by 51 ± 12%, the latter suggesting that denitrification may not have been the main source of emissions, contrary to the findings of Warneke et al. (2011). For constructed wetlands, elevated water tables are associated with a decrease in CO_2–C emission, highlighting the significance of anaerobic processes, which may have been the driver of CO_2–C emissions from the bioreactor.

4. Conclusions

This study provides a unique assessment of bioreactor performance at the lower boundary of N inputs. Understanding performance under low N loading is relevant not only to cropping and drainage systems with relatively low N export, but, perhaps more importantly, informs expectations for N removal efficiency in bioreactors used in conjunction with drainage water management, which alone can reduce N losses from fields by 17–80% (Skaggs et al., 2010), or other practices such as conservation tillage. Low pH and site constraints necessitating suboptimal bed dimensions may have also suppressed removal. Managing bed pH may be important for bioreactor applications with acidic agricultural drainage to enhance N removal and mitigate N_2O emissions, although concerning rates of GHG flux were not observed in this system. Conceptualizing how regional differences impact in-bed controls on N removal will guide adaptation of bioreactor designs to a wider range of agroecosystems, ultimately contributing to water quality improvement goals. Although bioreactor effectiveness relies on site-specific design, regional difference in artificial drainage networks, cropping systems, soil types, and hydrologic regimes can inform assessment of bioreactor utility and cost-effectiveness in the Mid-Atlantic.

Acknowledgements

This work was funded by a USDA-NRCS Conservation Innovation Grant #69-3A75-13-232.

Appendix A. Supplementary data

Supplementary data related to this article can be found at https://doi.org/10.1016/j.jenvman.2018.03.111.

References

Addy, K., Gold, A.J., Christianson, L.E., David, M.B., Schipper, L.A., Ratigan, N.A., 2016. Denitrifying bioreactors for nitrate removal: a meta-analysis. J. Environ. Qual. 45 (3), 873–881. https://doi.org/10.2134/jeq2015.07.0399.

Bock, E., Smith, N., Rogers, M., Coleman, B., Reiter, M., Benham, B., Easton, Z.M., 2015. Enhanced nitrate and phosphate removal in a denitrifying bioreactor with biochar. J. Environ. Qual. 44 (2), 605–613. https://doi.org/10.2134/jeq2014.03.0111.

Bock, E.M., Coleman, B., Easton, Z.M., 2016. Effect of biochar on nitrate removal in a pilot-scale denitrifying bioreactor. J. Environ. Qual. 45 (3), 762–771. https://doi.org/10.2134/jeq2015.04.0179.

Burke, P.M., Hill, S., Iricanin, N., Douglas, C., Essex, P., Tharin, D., 2002. Evaluation of preservation methods for nutrient species collected by automatic samplers. Environ. Monit. Assess. 80 (2), 149–173. https://doi.org/10.1023/A:1020660124582.

Christianson, L.E., Hedley, M., Camps, M., Free, H., Saggar, S., 2011. Influence of Biochar Amendements on Denitrificaiton Bioreactor Performance. Report. Massey University. Available: http://www.massey.ac.nz/~flrc/workshops/11/Manuscripts/Christianson_2011.pdf. (Accessed 6 February 2018).

Christianson, L., Bhandari, A., Helmers, M., Kult, K., Sutphin, T., Wolf, R., 2012. Performance and evaluation of four field-scale agricultural drainage denitrification bioreactors in Iowa. Trans. ASABE 55 (6), 2163–2174.

Christianson, L.E., Christianson, R., Helmers, M., Pederson, C., Bhandari, A., 2013a. Modeling and calibration of drainage denitrification bioreactor design criteria. J. Irrig. Drain. Eng. 139 (9), 699–709. https://doi.org/10.1061/(ASCE)IR.1943-4774.0000622.

Christianson, L.E., Helmers, M., Bhandari, A., Moorman, T., 2013b. Internal

hydraulics of an agricultural drainage denitrification bioreactor. Ecol. Eng. 52, 298–307. https://doi.org/10.1016/j.ecoleng.2012.11.001.
Christianson, L.E., Collick, A.S., Bryant, R.B., Rosen, T., Bock, E.M., Allen, A.L., Kleinman, P.J.A., May, E.B., Buda, A.R., Robinson, J., Folmar, G.J., Easton, Z.M., 2017. Enhanced denitrification bioreactors hold promise for Mid-Atlantic ditch drainage. Agric. Environ. Lett. 2, 170032 https://doi.org/10.2134/ael2017.09.0032.
Collier, S.M., Ruark, M.D., Oates, L.G., Jokela, W.E., Dell, C.J., 2014. Measurement of greenhouse gas flux from agricultural soils using static chambers. J. Vis. Exp. 90, e52110. https://doi.org/10.3791/52110.
David, M.B., Flint, C.G., Gentry, L.E., Dolan, M.K., Czapar, G.F., Cooke, R.A., Lavaire, T., 2015. Navigating the socio-bio-geo-chemistry and engineering of nitrogen management in two Illinois tile-drained watersheds. J. Environ. Qual. 44 (2), 368–381. https://doi.org/10.2134/jeq2014.01.0036.
de Klein, C.A.M., Harvey, M.J., 2012. Nitrous Oxide Chamber Methodology Guidelines–version 1.1. Global Research Alliance on Agricultural Greenhouse Gases. Available: https://globalresearchalliance.org/wp-content/uploads/2015/11/Chamber_Methodology _Guidelines_FinaL-V1.1-2015.pdf. (Accessed 10 December 2017).
Dinnes, D.L., Karlen, D.L., Jaynes, D.B., Kaspar, T.C., Hatfield, J.L., Colvin, T.S., Cambardella, C.A., 2002. Nitrogen management strategies to reduce nitrate leaching in tile-drained Midwestern soils. Agron. J. 94 (1), 153–171. https://doi.org/10.2134/agronj2002.1530.
Duran, B.E.L., Kucharik, C.J., 2013. Comparison of two chamber methods for measuring soil trace-gas fluxes in bioenergy cropping systems. Soil Sci. Soc. Am. J. 77 (5), 1601–1612. https://doi.org/10.2136/sssaj2013.01.0023.
Easton, Z.M., Rogers, M., Davis, M., Wade, J., Eick, M., Bock, E., 2015. Mitigation of sulfate reduction and nitrous oxide emission in denitrifying environments with amorphous iron oxide and biochar. Ecol. Eng. 82, 605–613. https://doi.org/10.1016/j.ecoleng.2015.05.008.
Elgood, Z., Robertson, W.D., Schiff, S.L., Elgood, R., 2010. Nitrate removal and greenhouse gas production in a stream-bed denitrifying bioreactor. Ecol. Eng. 36, 1575–1580. https://doi.org/10.1016/j.ecoleng.2010.03.011.
Gelman, A., Hill, J., 2007. Data Analysis Using Regression and Multilevel/Hierarchical Models. Cambridge University Press, New York, NY, p. 46.
Ghane, E., Ranaivoson, A.Z., Feyereisen, G.W., Rosen, C.J., Moncrief, J.F., 2016. Comparison of contaminant transport in agricultural drainage water and urban stormwater runoff. PLOS One 11 (12), e0167834. https://doi.org/10.1371/journal.pone.0167834.
Greenan, C.M., Moorman, T.B., Parkin, T.B., Kaspar, T.C., Jaynes, D.B., 2009. Denitrification in wood chip bioreactors at different water flows. J. Environ. Qual. 38 (4), 1664–1671. https://doi.org/10.2134/jeq2008.0413.
Hassanpour, B., Giri, S., Pluer, W.T., Steenhuis, T.S., Geohring, L.D., 2017. Seasonal performance of denitrifying bioreactors in the Northeastern United States: field trials. J. Environ. Manag. 202 (1), 224–253. https://doi.org/10.1016/j.jenvman.2017.06.054.
IA EPA, 2015. Illinois nutrient Loss Reduction Strategy. Springfield, IL. Available: http://www.epa.illinois.gov/assets/iepa/water-quality/watershed-management/nlrs/nlrsfinaL-revised-083115.pdf. (Accessed 11 December 2017).
IDALS, 2014. Iowa nutrient Reduction Strategy: a Science and Technology-based Framework to Assess and Reduce Nutrients to Iowa Waters and the Gulf of Mexico. Iowa Department of Agriculture and Land Stewardship, Iowa Department of Natural Resources, and Iowa State University. Available: http://www.nutrientstrategy.iastate.edu/. (Accessed 11 December 2017).
Ikenberry, C.D., Soupir, M.L., Schilling, K.E., Jones, C.S., Seeman, A., 2014. Nitrate-nitrogen export: magnitude and patterns from drainage districts to downstream river basins. J. Environ. Qual. 43 (6), 2024–2033. https://doi.org/10.2134/jeq2014.05.0242.
IPCC, 2007. In: Core Writinng Team, Pachauri, R.K., Reisinger, A. (Eds.), Contribution of Working Groups I, II, and III to the Fourth Assessment Report of the Intergovernmental Panel on Climate Change.
Kutzbach, L., Schneider, J., Sachs, T., Giebels, M., Nykänen, H., Shurpali, N.J., Martikainen, P.J., Alm, J., Wilmking, M., 2007. CO_2 flux determination by closed-chamber methods can be seriously biased by inappropriate application of linear regression. Biogeosciences 4, 1005–1025. https://doi.org/10.5194/bg-4-1005-2007.
Livingston, G.P., Hutchinson, G.L., Spartalian, Kevork, N.D., 2006. Trace gas emission in chambers: a non-steady-state diffusion model. Soil Sci. Soc. Am. J. 70 (5), 1459–1469. https://doi.org/10.2136/sssaj2005.0322.
Mander, U., Dotro, G., Ebie, Y., Towprayoon, S., Chiemchaisri, C., Nogueira, S.F., Jamsranjav, B., Kasak, K., Truu, J., Tournebize, J., Mitsch, W.J., 2014. Greenhouse gas emission in constructed wetlands for wastewater treatment: a review. Ecol. Eng. 66, 19–35. https://doi.org/10.1016/j.ecoleng.2013.12.006.
Mateju, V., Cizinska, S., Krejci, J., Janock, T., 1992. Biological water denitrificaiton - a reivew. Enzyme Microb. Technol. 14 (3), 170–183. https://doi.org/10.1016/0141-0229(92)90062-S.
MN PCA, 2014. The Minnesota Nutrient Reduction Strategy. Minnesota Pollution Control Agency, St. Paul, MN. Available: https://www.pca.state.mn.us/sites/default/files/wq-s1-80.pdf. (Accessed 11 December 2017).
Moorman, T.B., Parkin, T.B., Kaspar, T.C., Jaynes, D.B., 2010. Denitrification activity, wood loss, and N_2O emissions over 9 years from a wood chip bioreactor. Ecol. Eng. 36, 1567–1574. https://doi.org/10.1016/j.ecoleng.2010.03.012.
Partheeban, C., Karkl, G., Khand, K.B., Kjaersgaard, J., Hay, C., Troolen, T., 2014. Calibration of AgriDrain control structure by using generalized. In: "V" Notch Weir Equation for Flow Measurement. Western South Dakota Hydrology Conference. Available: https://www.researchgate.net/publication/276832543_Calibration_of_AgriDrain_control_structure_by_using_generalized_V_notch_weir_equation_for_flow_measurement. (Accessed 12 December 2017).
Pluer, W.T., Geohring, L.D., Steenhuis, T.S., Walter, M.T., 2016. Controls influencing the treatment of excess agricultural nitrate with denitrifying bioreactors. J. Environ. Qual. 45 (3), 772–778. https://doi.org/10.2134/jeq2015.06.0271.
R Core Team, 2017. R: a Language and Environment for Statistical Computing. R Foundation for Statistical Computing, Vienna, Austria. Available: http://www.R-project.org/>. (Accessed 12 December 2017).
Rosen, T., Christianson, L., 2017. Performance of denitrifying bioreactors at reducing agricultural nitrogen pollution in a humid subtropical coastal plain climate. Water 9 (2), 112. https://doi.org/10.3390/w9020112.
Schipper, L.A., Robertson, W.D., Gold, A.J., Jaynes, D.B., Cameron, S.C., 2010. Denitrifying bioreactors—an approach for reducing nitrate loads to receiving waters. Ecol. Eng. 36, 1532–1543. https://doi.org/10.1016/j.ecoleng.2010.04.008.
Skaggs, R., Youssef, M., Gilliam, J., Evans, R., 2010. Effect of controlled drainage on water and nitrogen balances in drained lands. Trans. ASABE. 53 (6), 1843–1850. https://doi.org/10.13031/2013.35810.
Soil Survey Staff, Natural Resources Conservation Service, United States Department of Agriculture. Web Soil Survey. <https://websoilsurvey.sc.egov.usda.gov/> (accessed April 6, 2017).
USDA NASS, 2012. Census of Agriculture, Ag Census Web Maps. Available: www.agcensus.usda.gov/Publications/2012/Online_Resources/Ag_Census_Web_Maps/Overview/. (Accessed 6 February 2018).
USDA-NRCS, 2015. Conservation Practice Standard Denitrifying Bioreactor Code 605 (605-CPS-1). USDA-NRCS, Washington, DC.
van Driel, P.P.W., Robertson, W.W.D., Merkley, L.L.C., 2006. Denitrification of agricultural drainage using wood-based reactors. Trans. ASABE. 49 (2), 565–573. https://doi.org/10.13031/2013.20391.
Warneke, S., Schipper, L.A., Bruesewitz, D.A., McDonald, I., Cameron, S., 2011. Rates, controls and potential adverse effects of nitrate removal in a denitrification bed. Ecol. Eng. 37 (3), 511–522. https://doi.org/10.1016/j.ecoleng.2010.12.006.
Williams, M.R., King, K.W., Fausey, N.R., 2015. Drainage water management effects on tile discharge and water quality. Agric. Water Manag. 148, 45–51. https://doi.org/10.1016/j.agwat.2014.09.017.
Woli, K.P., David, M.B., Cooke, R.A., McIsaac, G.F., Mitchell, C.A., 2010. Nitrogen balance in and export from agricultural fields associated with controlled drainage systems and denitrifying bioreactors. Ecol. Eng. 36 (11), 1558–1566. https://doi.org/10.1016/j.ecoleng.2010.04.024.